

## It is Feasible to Directly Measure Black Hole Masses in the First Galaxies

HAMSA PADMANABHAN<sup>1</sup> AND ABRAHAM LOEB<sup>2</sup>

<sup>1</sup>*Canadian Institute for Theoretical Astrophysics  
60 St. George Street, Toronto, ON M5S 3H8, Canada*

<sup>2</sup>*Astronomy department, Harvard University  
60 Garden Street, Cambridge, MA 02138, USA*

### ABSTRACT

In the local universe, black hole masses have been inferred from the observed increase in the velocities of stars at the centres of their host galaxies. So far, masses of supermassive black holes in the early universe have only been inferred indirectly, using relationships calibrated to their locally observed counterparts. Here, we use the latest observational constraints on the evolution of stellar masses in galaxies to predict that the region of influence of a central supermassive black hole at the epochs where the first galaxies were formed is *directly resolvable* by current and upcoming telescopes. Such measurements will usher in a new era of discoveries unraveling the formation of the first supermassive black holes based on subarcsecond-scale spectroscopy with the *ALMA*<sup>a)</sup>, *JWST*<sup>b)</sup> and the *SKA*. The measured mass distribution of black holes will allow forecasting of the future detection of gravitational waves from the earliest black hole mergers.

### 1. INTRODUCTION

Massive black holes (with masses of about a million solar masses) are known to exist at the centres of galaxies in the nearby universe. Locally, the masses of such black holes have been measured from their gravitational radius of influence on the motion of stars and gas in their host galaxies. This method was particularly effective for the Milky Way (Ghez et al. 2005, 2008; Genzel et al. 2000; Schödel et al. 2003) and NGC 4258 (Miyoshi et al. 1995). Local measurements imply a ratio of the central black hole mass to stellar mass  $M_*$  of the host spheroid to be about  $10^{-4} - 10^{-3}$  in the local universe (Kormendy & Ho 2013; Reines & Volonteri 2015).

Supermassive black holes with masses  $M_{\text{BH}}$  of more than a billion solar masses are inferred to exist out to a redshift  $z = 7.54$ , less than  $\sim 700$  million years after the Big Bang (Bañados et al. 2018). How the seeds for these black holes grew so early in the universe is still an open question (Inayoshi et al. 2019). However, there is evidence indicating that at redshifts  $z > 6$ , the central black hole to stellar mass ratio had been more than order of magnitude or two higher (Decarli et al. 2018; Venemans et al. 2016) than the locally observed value. Theoretical arguments supporting this evolution stem from the inferred black hole - bulge mass relation (Wyithe & Loeb 2002a; Croton 2009) extrapolated to high redshifts, suggesting that  $M_{\text{BH}}$  grows as a steep function of the halo circular velocity  $v_c$ :  $M_{\text{BH}} \propto v_c^\gamma$  with  $\gamma \sim 5$ .

The evolution of the stellar mass  $M_*$  in dark matter haloes of both early and present-day galaxies is fairly well-constrained. The latest observations from a wide range of surveys, including the Sloan Digital Sky Survey (SDSS), the PRISM Multi-object Survey (PRIMUS), UltraVISTA, the Cosmic Assembly Near-infrared Deep Extragalactic Legacy Survey (CANDELS), and the FourStar Galaxy Evolution Survey (ZFOURGE) all support (Behroozi et al. 2019) a well-defined  $M_*(z)$  across the full redshift range,  $0 < z < 10.5$ . The data indicate that the average stellar mass in Milky-Way sized dark matter haloes evolves only by a factor of  $\sim 1.6$  over redshifts  $z \sim 6$  to the present (see Fig. 9 of Behroozi et al. (2019)).

The above two results, taken together, imply a fascinating conclusion. Since the stellar mass evolves much more modestly than the black hole mass (a trend also found in recent AGN observations from the *Chandra*-COSMOS Legacy Survey; Suh et al. 2019), the central black hole mass makes up a much larger fraction of the stellar mass at high redshifts (a fraction of  $\sim 0.3$  at redshift  $z \sim 6$  compared to  $10^{-4}$  at  $z \sim 0$ ). This fact, already hinted at

hamsa@cita.utoronto.ca, aloeb@cfa.harvard.edu

<sup>a)</sup> <https://almascience.nrao.edu/about-alma/alma-basics>

<sup>b)</sup> <https://www.jwst.nasa.gov/>

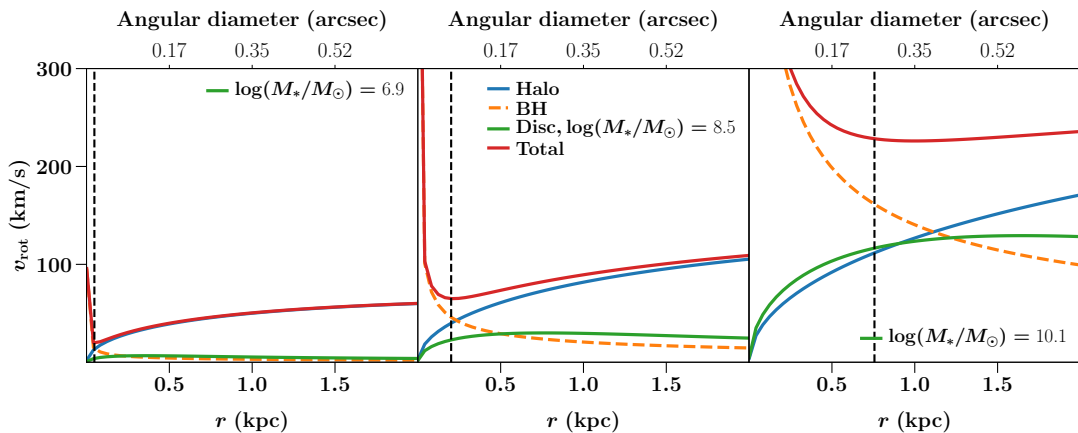


**Figure 1.** Rotation curves around three typical dark matter haloes (with masses  $M_{\text{halo}} = 10^{10}, 10^{11}$  and  $10^{12} M_{\odot}$  respectively from left to right) at  $z = 6$ . The halo is assumed to follow a Navarro-Frenk-White (Navarro et al. 1996) profile with a concentration parameter (Diemer & Joyce 2018)  $c = 3.5$ , and contains a central supermassive black hole, with mass  $M_{\text{BH}}$ , and an exponential stellar disc with spin parameter  $\lambda = 0.03$  (the inferred total stellar mass  $M_*$  is also indicated). The circular velocities  $v_{\text{rot}}$  (in km/s) induced by the black hole (orange dashed lines), stellar disc (green solid lines) and dark matter halo (blue solid lines) are plotted along with the total circular velocity (red solid line). The central dominance of the black hole leads to a visible Keplerian correction in the otherwise flat rotation curve within the inner  $< 1$  kpc. Dashed lines in each panel indicate  $R_{\text{inf}}$ , the radius of influence at which  $M_{\text{BH}} = M_{\text{halo}}(R_{\text{inf}}) + M_{\text{d}}(R_{\text{inf}})$ . Top horizontal axes show the angular diameter  $\theta = [2r/D_A(z)]$  corresponding to the radial distance  $r$  on the lower horizontal axis.

by pre-*ALMA* estimates (Davis 2014) and *ALMA* observations of  $z \sim 6.6 - 6.9$  galaxies (Venemans et al. 2016), is well-supported by the recent *ALMA* spectroscopic study (Decarli et al. 2018) of [CII]-detected quasars at  $z > 6$  which indicates significantly more than two orders of magnitude evolution of the locally observed black hole - bulge mass relation (Reines & Volonteri 2015). An immediate implication of this finding is that the central black hole should have a measurable influence on the circular velocity profiles of galaxies at high redshift.

To quantify this effect, we predict the rotation curves of typical Milky-Way sized haloes at  $z \sim 6$ , separating the dark matter, stellar disc, and black hole components. For the dark matter, we assume a Navarro-Frenk-White (Navarro et al. 1996; Mo et al. 1998) profile with the mass  $M_{\text{halo}}(r)$  within radius  $r$  given by Eq. (19) of Mo et al. (1998). The halo concentration is assumed to be  $c = 3.5$  at  $z = 6$ , consistent with the findings of the recent physically motivated models (Diemer & Joyce 2018). For the stellar component, we use an exponential disc profile as defined in Eq. (5) of Mo et al. (1998), assuming that the stellar mass resides primarily in the disc ( $m_d = M_*/M_{\text{halo}}$ , with  $M_*$  being the average stellar mass  $M_*$  in the halo from Behroozi et al. (2019) with a non-evolving specific angular momentum parameter ( $j_d/m_d \approx 1$ ) and spin parameter ( $\lambda = 0.03$ ). The disc masses within a distance  $r$  from the centre of the galaxy,  $M_d(r)$ , are computed from Eq. (26) of Mo et al. (1998)). The black hole is assumed to be a central point source with mass  $M_{\text{BH}}$  given by Wyithe & Loeb (2002a).

## 2. RESULTS

Figure 1 shows the above three components at  $z \sim 6$  for three representative dark matter haloes with masses  $M_{\text{halo}} = 10^{10}, 10^{11}$  and  $10^{12} M_{\odot}$ , respectively. The inferred total stellar masses  $M_*$  from Behroozi et al. (2019) are indicated on each panel. Our predicted disc radii evolve as  $(1+z)^\beta$  with  $\beta \approx -1$  for this stellar mass range, consistent with the findings from the CANDELS (Kawamata et al. 2018) and HST/Hubble Frontier Fields (Shibuya et al. 2019; Holwerda et al. 2015) galaxy observations at  $z \sim 6 - 8$ . The black hole masses in these galaxies predicted from Wyithe & Loeb (2002a) are  $\log_{10}(M_{\text{BH}}/M_{\odot}) = 6.3, 8.0, 9.7$ , implying  $M_{\text{BH}}/M_* \approx 0.3 - 0.4$ . The figure shows rotational circular velocities,  $v_{\text{rot},i} = (GM_i(r)/r)^{1/2}$  as a function of radial distance  $r$ , where  $i$  denotes the disc, black hole or halo component. The total circular velocity, given by  $v_{\text{tot}}(r) = (\sum_i v_{\text{rot},i}(r)^2)^{1/2}$  is also plotted. A Keplerian correction to the rotation curve at the innermost  $< 1$  kpc is clearly distinguishable for stellar masses of  $10^9 - 10^{10} M_{\odot}$ , a mass range for which sub-millimetre observations already exist in the literature (Shibuya et al. 2019). The radius of influence  $R_{\text{inf}}$  of the black hole, defined as the scale at which  $M_{\text{BH}} = M_d(R_{\text{inf}}) + M_{\text{halo}}(R_{\text{inf}})$ , is indicated by the dashed line on each panel. For the three galaxy masses considered,  $R_{\text{inf}}$  ranges from 0.05 to 0.76 kpc, corresponding to angular diameter

sizes,  $\theta = (2R_{\text{inf}}/D_A)$  of  $0.01''$ ,  $0.06''$  and  $0.26''$  respectively, where  $D_A$  is the cosmological angular-diameter distance to redshift  $z = 6$ .

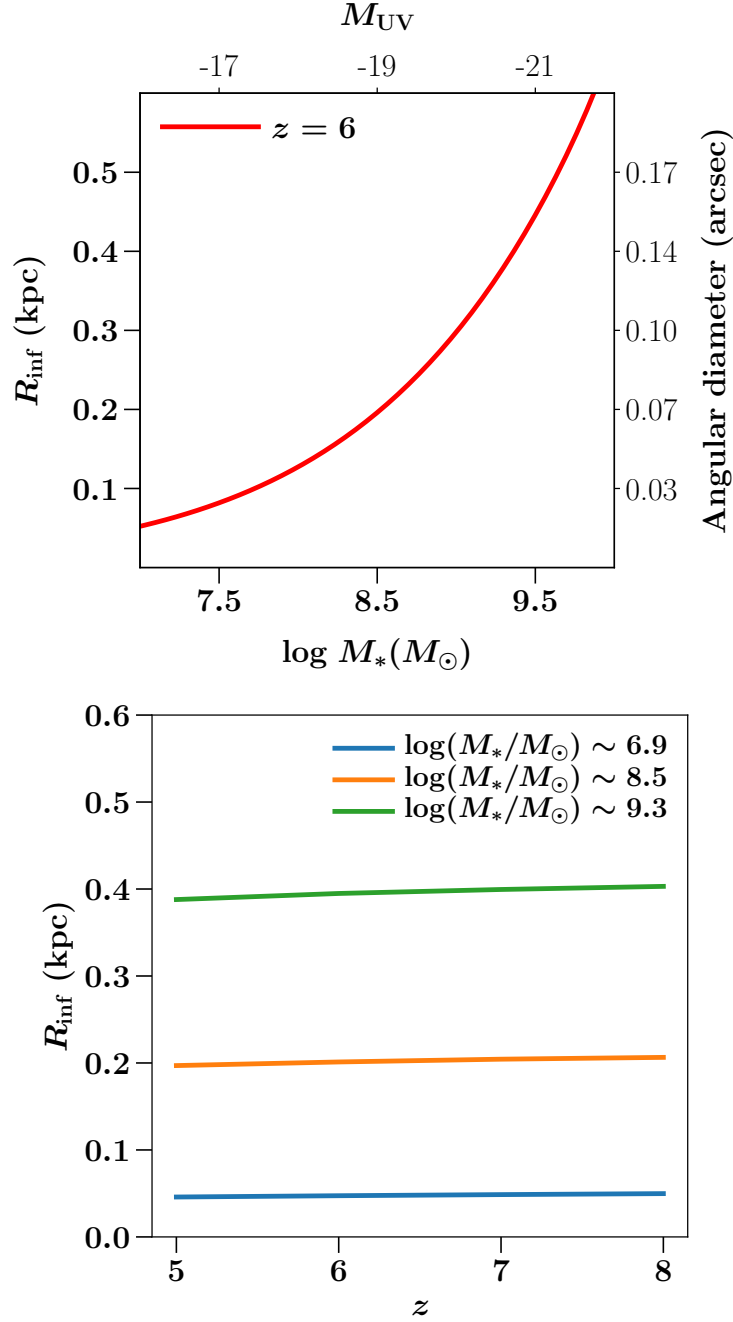


**Figure 2.** *Top panel:* Evolution of the radius of influence,  $R_{\text{inf}}$ , of the central black hole as a function of the surrounding stellar mass,  $M_*$  (lower horizontal axis) and the corresponding absolute magnitude,  $M_{\text{UV}}$  of the host galaxy (upper horizontal axis) at  $z = 6$ , assuming the same dark matter halo, stellar disc and central black hole properties as in Fig.1. The right-hand vertical axis indicates the corresponding angular diameter scale  $\theta = [2R_{\text{inf}}/D_A(z = 6)]$ . *Lower panel:* Evolution of the black hole radius of influence  $R_{\text{inf}}$  with  $z$  for three different halo masses ( $\log_{10}(M_{\text{halo}}/M_\odot) = 10, 11$  and  $11.5$  respectively, corresponding to the inferred stellar mass range  $\log_{10}(M_*/M_\odot) \approx 6.9 - 9.3$ ).

The evolution of  $R_{\text{inf}}$  with stellar mass and redshift is shown in Fig. 2. The top panel shows that  $R_{\text{inf}}$  evolves strongly with stellar masses in the range  $10^7 - 10^{10} M_{\odot}$  at  $z \sim 6$ , as can also be seen from Fig. 1. The absolute magnitudes ( $M_{\text{UV}}$  in the upper  $x$ -axis) corresponding to this mass range are computed from the observationally derived relation (Tacchella et al. 2018) at  $z = 6$ . The lower panel shows  $R_{\text{inf}}$  at three different halo masses ( $\log_{10}(M_{\text{halo}}/M_{\odot}) = 10, 11, 11.5$ ) across the range  $z \sim 5 - 8$ . This halo mass range corresponds to a stellar mass range of  $\log_{10}(M_*/M_{\odot}) \approx 6.9 - 9.3$ , which is accessible to HST at these redshifts (Holwerda et al. 2015). The near-constant black hole - stellar mass relation in this  $z$ -range implies that  $R_{\text{inf}}$  does not evolve much with redshift for a given halo mass.

For the highest stellar masses, the black hole can dominate the kinematics up to a distance  $> 0.5$  kpc, which corresponds to an angular scale of  $> 0.2''$ . These values are well within the reach of current and upcoming observations. *ALMA* in its extended 12-m configuration should be able to detect [CII]-emitting galaxies with  $0.02 - 0.043''$  resolution at frequencies corresponding to  $z \sim 6 - 10$ , and the future James Webb Space Telescope (*JWST*) should be able (Vogelsberger et al. 2019) to resolve at least  $\sim 200$  such galaxies at  $z \sim 8$ . Further, the *VLA*<sup>1</sup> and the Phase II of the planned Square Kilometre Array (SKA; Taylor 2013) will be able to access the CO J 1  $\rightarrow$  0 transition at redshifts  $z \sim 6 - 10$  with angular resolutions of  $0.2-0.3''$ , which could potentially resolve  $R_{\text{inf}}$  of the central black hole in the brightest galaxies at these epochs.

### 3. CONCLUSIONS

These predictions have far-reaching implications. First, a direct *kinematic* measurement of the central black hole masses will enable key physics insights into the growth and merger histories of supermassive black holes in the earliest galaxies. It would also shed light on the active phases ('duty cycles') of the earliest black holes, and permit exciting constraints on the currently debated contribution of quasars to cosmic reionization of hydrogen and helium (Madau & Haardt 2015). It has been recently suggested that a significant population of strongly lensed quasars (Fan et al. 2019; Wyithe & Loeb 2002b) in the early universe may have been missed by current surveys due to selection effects that rule out bright lenses (Pacucci & Loeb 2019). Direct black hole mass measurements form a complementary dataset to aid detections of lensed quasars from future surveys. Finally, a characterization of the black hole mass function will enable forecasting of future measurements of gravitational radiation emitted by pairs of these produced by galaxy mergers (Goulding et al. 2019), in anticipation of the upcoming Laser Interferometer Space Antenna (*LISA*)<sup>2</sup>.

### ACKNOWLEDGEMENTS

This work was supported in part by Harvard's Black Hole Initiative, which is funded by grants from JTF and GBMF.

### REFERENCES

- Bañados, E., Venemans, B. P., Mazzucchelli, C., et al. 2018, *Nature*, 553, 473, doi: [10.1038/nature25180](https://doi.org/10.1038/nature25180)
- Behroozi, P., Wechsler, R. H., Hearin, A. P., & Conroy, C. 2019, *MNRAS*, 488, 3143, doi: [10.1093/mnras/stz1182](https://doi.org/10.1093/mnras/stz1182)
- Croton, D. J. 2009, *MNRAS*, 394, 1109, doi: [10.1111/j.1365-2966.2009.14429.x](https://doi.org/10.1111/j.1365-2966.2009.14429.x)
- Davis, T. A. 2014, *MNRAS*, 443, 911, doi: [10.1093/mnras/stu1163](https://doi.org/10.1093/mnras/stu1163)
- Decarli, R., Walter, F., Venemans, B. P., et al. 2018, *The Astrophysical Journal*, 854, 97, doi: [10.3847/1538-4357/aaa5aa](https://doi.org/10.3847/1538-4357/aaa5aa)
- Diemer, B., & Joyce, M. 2018, arXiv e-prints, arXiv:1809.07326. <https://arxiv.org/abs/1809.07326>
- Fan, X., Wang, F., Yang, J., et al. 2019, *ApJ*, 870, L11, doi: [10.3847/2041-8213/aaeffe](https://doi.org/10.3847/2041-8213/aaeffe)
- Genzel, R., Pichon, C., Eckart, A., Gerhard, O. E., & Ott, T. 2000, *MNRAS*, 317, 348, doi: [10.1046/j.1365-8711.2000.03582.x](https://doi.org/10.1046/j.1365-8711.2000.03582.x)
- Ghez, A. M., Salim, S., Hornstein, S. D., et al. 2005, *ApJ*, 620, 744, doi: [10.1086/427175](https://doi.org/10.1086/427175)
- Ghez, A. M., Salim, S., Weinberg, N. N., et al. 2008, *ApJ*, 689, 1044, doi: [10.1086/592738](https://doi.org/10.1086/592738)
- Goulding, A. D., Pardo, K., Greene, J. E., et al. 2019, *ApJ*, 879, L21, doi: [10.3847/2041-8213/ab2a14](https://doi.org/10.3847/2041-8213/ab2a14)
- Holwerda, B. W., Bouwens, R., Oesch, P., et al. 2015, *ApJ*, 808, 6, doi: [10.1088/0004-637X/808/1/6](https://doi.org/10.1088/0004-637X/808/1/6)
- Inayoshi, K., Visbal, E., & Haiman, Z. 2019, arXiv e-prints, arXiv:1911.05791. <https://arxiv.org/abs/1911.05791>
- Kawamata, R., Ishigaki, M., Shimasaku, K., et al. 2018, *ApJ*, 855, 4, doi: [10.3847/1538-4357/aaa6cf](https://doi.org/10.3847/1538-4357/aaa6cf)

<sup>1</sup> <https://science.nrao.edu/facilities/vla/>

<sup>2</sup> <https://www.lisamission.org>

- Kormendy, J., & Ho, L. C. 2013, *ARA&A*, 51, 511,  
doi: [10.1146/annurev-astro-082708-101811](https://doi.org/10.1146/annurev-astro-082708-101811)
- Madau, P., & Haardt, F. 2015, *ApJ*, 813, L8,  
doi: [10.1088/2041-8205/813/1/L8](https://doi.org/10.1088/2041-8205/813/1/L8)
- Miyoshi, M., Moran, J., Herrnstein, J., et al. 1995, *Nature*,  
373, 127, doi: [10.1038/373127a0](https://doi.org/10.1038/373127a0)
- Mo, H. J., Mao, S., & White, S. D. M. 1998, *MNRAS*, 295,  
319, doi: [10.1046/j.1365-8711.1998.01227.x](https://doi.org/10.1046/j.1365-8711.1998.01227.x)
- Navarro, J. F., Frenk, C. S., & White, S. D. M. 1996, *ApJ*,  
462, 563, doi: [10.1086/177173](https://doi.org/10.1086/177173)
- Pacucci, F., & Loeb, A. 2019, *ApJ*, 870, L12,  
doi: [10.3847/2041-8213/aaf86a](https://doi.org/10.3847/2041-8213/aaf86a)
- Reines, A. E., & Volonteri, M. 2015, *ApJ*, 813, 82,  
doi: [10.1088/0004-637X/813/2/82](https://doi.org/10.1088/0004-637X/813/2/82)
- Schödel, R., Ott, T., Genzel, R., et al. 2003, *ApJ*, 596,  
1015, doi: [10.1086/378122](https://doi.org/10.1086/378122)
- Shibuya, T., Ouchi, M., Harikane, Y., & Nakajima, K.  
2019, *ApJ*, 871, 164, doi: [10.3847/1538-4357/aaf64b](https://doi.org/10.3847/1538-4357/aaf64b)
- Suh, H., Civano, F., Trakhtenbrot, B., et al. 2019, arXiv  
e-prints, arXiv:1912.02824.  
<https://arxiv.org/abs/1912.02824>
- Tacchella, S., Bose, S., Conroy, C., Eisenstein, D. J., &  
Johnson, B. D. 2018, *ApJ*, 868, 92,  
doi: [10.3847/1538-4357/aae8e0](https://doi.org/10.3847/1538-4357/aae8e0)
- Taylor, A. R. 2013, in *IAU Symposium*, Vol. 291, *Neutron  
Stars and Pulsars: Challenges and Opportunities after 80  
years*, ed. J. van Leeuwen, 337–341,  
doi: [10.1017/S1743921312024039](https://doi.org/10.1017/S1743921312024039)
- Venemans, B. P., Walter, F., Zschaechner, L., et al. 2016,  
*ApJ*, 816, 37, doi: [10.3847/0004-637X/816/1/37](https://doi.org/10.3847/0004-637X/816/1/37)
- Vogelsberger, M., Nelson, D., Pillepich, A., et al. 2019,  
arXiv e-prints, arXiv:1904.07238.  
<https://arxiv.org/abs/1904.07238>
- Wyithe, J. S. B., & Loeb, A. 2002a, *ApJ*, 581, 886,  
doi: [10.1086/344249](https://doi.org/10.1086/344249)
- Wyithe, J. S. B., & Loeb, A. 2002b, *Nature*, 417, 923,  
doi: [10.1038/nature00794](https://doi.org/10.1038/nature00794)